

Evidence for 3D-xy critical properties in underdoped  $\text{YBa}_2\text{Cu}_3\text{O}_{7-\delta}$ T. Schneider<sup>1,\*</sup><sup>1</sup>*Physik-Institut der Universität Zürich, Winterthurerstrasse 190, CH-8057, Switzerland*

We perform a detailed analysis of the irreversible magnetization data of Salem-Sugui *et al.* and Babic *et al.* of underdoped and optimally doped  $\text{YBa}_2\text{Cu}_3\text{O}_{7-\delta}$  single crystals. Near the zero field transition temperature we observe extended consistency with the properties of the 3D-xy universality class, even though the attained critical regime is limited by an inhomogeneity induced finite size effect. Nevertheless, as  $T_c$  falls from 93.5 to 41.5 K the critical amplitude of the in-plane correlation length  $\xi_{ab0}$ , the anisotropy  $\gamma = \xi_{ab0}/\xi_{c0}$  and the critical amplitude of the in-plane penetration depth  $\lambda_{ab0}$  increase substantially, while the critical amplitude of the  $c$ -axis correlation length  $\xi_{c0}$  does not change much. As a consequence, the correlation volume  $V_{corr}^-$  increases and the critical amplitude of the specific heat singularity  $A^-$  decreases dramatically, while the rise of  $\lambda_{ab0}$  reflects the behavior of the zero temperature counterpart. Conversely, although  $\xi_{ab0}$  and  $\lambda_{ab0}$  increase with reduced  $T_c$ , the ratio  $\lambda_{ab0}/\xi_{ab0}^-$ , corresponding to the Ginzburg-Landau parameter  $\kappa_{ab}$ , decreases substantially and  $\text{YBa}_2\text{Cu}_3\text{O}_{7-\delta}$  crosses over from an extreme to a weak type-II superconductor.

PACS numbers: 74.25.Bt, 74.25.Ha, 74.40.+k

Since the discovery of cuprate superconductors, fluctuation contributions to the specific heat, magnetization, magnetic penetration depths etc. have been measured in a variety of compounds. In principle, fluctuation studies yield such important information as the universality class onto which these superconductors fall and their effective dimensionality.<sup>1,2</sup> Given the universality class, various properties, e.g. the correlation volume above and below  $T_c$ , are no longer independent but related in terms of universal coefficients. As a consequence, the isotope and pressure effects on various properties are no longer independent.<sup>3</sup> In nearly optimally doped  $\text{YBa}_2\text{Cu}_3\text{O}_{7-\delta}$ ,  $\text{HgBa}_2\text{CuO}_{4-\delta}$  and  $\text{La}_{2-x}\text{Sr}_x\text{CuO}_4$  the occurrence of 3D-xy criticality is reasonably well established.<sup>4,5,6</sup> However, in the underdoped regime the anisotropy increases with reduced  $T_c$ .<sup>7</sup> Although reduced dimensionality is accompanied with enhanced fluctuations the 3D-xy critical regime is expected to shrink. Nevertheless, consistency with 3D-xy scaling was observed in magnetization measurements of  $\text{YBa}_2\text{Cu}_3\text{O}_{7-\delta}$  down to  $T_c \simeq 61.4$  K.<sup>5</sup> On the other hand, measurements of the magnetic penetration depth uncovered charged critical behavior in  $\text{YBa}_2\text{Cu}_3\text{O}_{6.95}$  sample with  $T_c \simeq 61.4$  K.<sup>8</sup> Note that  $7 - \delta = 6.95$  is close to the hole concentration  $p \simeq 1/8$  where charge fluctuations are important.<sup>9</sup>

Recently, magnetization measurements have been performed on underdoped  $\text{YBa}_2\text{Cu}_3\text{O}_{7-\delta}$  single crystals with  $T_c \simeq 41.5$  K and  $T_c \simeq 62$  K by Salem-Sugui *et al.*<sup>10,11</sup> Here we perform a detailed analysis of these data. In contrast to previous work<sup>4,5</sup> we do not establish the consistency with the 3D-xy scaling plots only, but estimate, given the critical exponent of the correlation lengths,  $\nu \simeq 2/3$ , the critical amplitudes of the correlation length, the universal ratios, etc., of the associated fictitious homogeneous system as well. Indeed, the universality class to which a given experimental system belongs is not only characterized by its critical exponents but also by various critical point amplitude ratios and universal coefficients. This is achieved by invoking the

limiting behavior of the universal scaling function, allowing to explore the growth of the in-plane and  $c$ -axis correlation lengths as  $T_c$  is approached. The observed limitations of this growth are traced back to a finite size effect, whereupon the correlation lengths cannot grow beyond the extent of the homogeneous domains. Clearly, such an analysis does not discriminate between intrinsic or extrinsic inhomogeneities, but it provides lower bounds for the extent of the homogeneous domains seen by the relevant fluctuations.

The paper is organized as follows: Next we present a short sketch of the scaling theory and the universal properties appropriate of anisotropic extreme type-II superconductor exhibiting in the absence of an applied magnetic field 3D-xy criticality. On this basis we analyze the irreversible magnetization data of Salem-Sugui *et al.*<sup>10,11</sup> and Babic *et al.*<sup>5</sup> We observe close to the zero field  $T_c$  remarkable consistency with the scaling and critical properties of a finite system belonging to the 3D-xy universality class. Indeed, the homogeneity of the samples turns out to be of finite extent, preventing the correlation lengths to grow beyond the extent of the homogeneous regions. Accordingly, the magnetization data does not provide estimates of the scaling and critical properties only, but uncovers the spatial extent of the homogeneous regions as well. As  $T_c$  falls from 93.5 to 41.5 K we observe that the critical amplitude of the in-plane correlation length  $\xi_{ab0}$ , the anisotropy  $\gamma = \xi_{ab0}/\xi_{c0}$  and the critical amplitude of the in-plane penetration depth  $\lambda_{ab0}$  increase substantially, while the critical amplitude of the  $c$ -axis correlation length does not change much. As a consequence, the correlation volume  $V_{corr}^-$  increases and the critical amplitude of the specific heat singularity  $A^-$  decreases dramatically, while the rise of  $\lambda_{ab0}$  reflects the behavior of the zero temperature counterpart.<sup>12</sup> Conversely, although  $\xi_{ab0}$  and  $\lambda_{ab0}$  increase with reduced  $T_c$ , the ratio  $\lambda_{ab0}/\xi_{ab0}^-$ , corresponding to the Ginzburg-Landau parameter  $\kappa_{ab}$ , decreases substantially and  $\text{YBa}_2\text{Cu}_3\text{O}_{7-\delta}$  crosses over from an extreme to a weak type-II superconductor.

ductor. The rise of the anisotropy with reduced  $T_c$  is consistent with a previous magnetic torque study<sup>13</sup>. For the extent of the homogenous domains we derive from the finite size effect in  $\xi_{ab}$  and  $\xi_c$  the lower bounds  $L_{ab} \simeq 367 \text{ \AA}$ ,  $L_c \simeq 53 \text{ \AA}$  and  $L_{ab} \simeq 254 \text{ \AA}$ ,  $L_c \simeq 53 \text{ \AA}$  for the samples of Salem-Sugui *et al.*<sup>10,11</sup> with  $T_c \simeq 41.5$  and  $T_c \simeq 62$  K, respectively.

To derive the scaling form of the magnetization in the fluctuation dominated regime we note that the scaling of the magnetic field is in terms of the number of flux quanta per correlation area. Thus, when the thermal fluctuations of the order parameter dominate the singular part of the free energy per unit volume of a homogeneous system scales as<sup>1,2,6,14,15,16,17,18</sup>

$$f_s = \frac{Q^\pm k_B T}{\xi_{ab}^2 \xi_c} G(z) = \frac{Q^\pm k_B T \gamma}{\xi_{ab}^3} G(z), \quad z = \frac{H \xi_{ab}^2}{\Phi_0}. \quad (1)$$

$Q^\pm$  is a universal constant and  $G^\pm(z)$  a universal scaling function of its argument, with  $G^\pm(z=0) = 1$ .  $\gamma = \xi_{ab}/\xi_c$  denotes the anisotropy,  $\xi_{ab}$  the zero-field in-plane correlation length and  $H$  the magnetic field applied along the  $c$ -axis. Approaching  $T_c$  the in-plane correlation length diverges as

$$\xi_{ab} = \xi_{ab0}^{\pm} |t|^{-\nu}, \quad t = T/T_c - 1, \quad \pm = \text{sgn}(t). \quad (2)$$

Supposing that 3D-xy fluctuations dominate the critical exponents are given by<sup>19</sup>

$$\nu \simeq 0.671 \simeq 2/3, \quad \alpha = 2\nu - 3 \simeq -0.013, \quad \nu \simeq 0.671, \quad (3)$$

and there are the universal critical amplitude relations<sup>1,2,14,15,16,19</sup>

$$\frac{\xi_{ab0}^-}{\xi_{ab0}^+} = \frac{\xi_{c0}^-}{\xi_{c0}^+} \simeq 2.21, \quad \frac{Q^-}{Q^+} \simeq 11.5, \quad \frac{A^+}{A^-} = 1.07, \quad (4)$$

and

$$A^- (\xi_{ab0}^-)^2 \xi_{c0}^- = \frac{A^- (\xi_{ab0}^-)^3}{\gamma} = (R^-)^3, \quad R^- \simeq 0.815, \quad (5)$$

where  $A^\pm$  is the critical amplitude of the specific heat singularity, defined as  $c = (A^\pm/\alpha) |t|^{-\alpha} + B$ . Furthermore, in the 3D-xy universality class  $T_c$ ,  $\xi_{c0}^-$  and the critical amplitude of the in-plane penetration depth  $\lambda_{ab0}$  are not independent but related by the universal relation<sup>1,2,14,15,16,19</sup>,

$$k_B T_c = \frac{\Phi_0^2}{16\pi^3} \frac{\xi_{c0}^-}{\lambda_{ab0}^2} = \frac{\Phi_0^2}{16\pi^3} \frac{\xi_{ab0}^-}{\gamma \lambda_{ab0}^2}. \quad (6)$$

From the singular part of the free energy per unit volume given by Eq. (1) we derive for the magnetization per unit volume  $m = M/V = -\partial f_s / \partial H$  the scaling form

$$\frac{m}{T H^{1/2}} = -\frac{Q^\pm k_B \gamma}{\Phi_0^{3/2}} F(z), \quad F^\pm(z) = z^{-1/2} \frac{dG}{dz}, \quad (7)$$

where

$$z = \frac{\xi_{ab}^2}{a L_{H_c}^2} = x^{-1/2\nu} = \frac{(\xi_{ab0}^\pm)^2 |t|^{-2\nu} H}{\Phi_0}.$$

This scaling form is similar to Prange's<sup>20</sup> result for Gaussian fluctuations. More generally, the existence of the magnetization at  $T_c$ , of the penetration depth below  $T_c$  and of the magnetic susceptibility above  $T_c$  imply the following asymptotic forms of the scaling function<sup>1,2,6,17,18</sup>

$$Q^\pm \left. \frac{1}{\sqrt{z}} \frac{dG}{dz} \right|_{z \rightarrow \infty} = Q^\pm c_\infty^\pm, \quad Q^- \left. \frac{dG}{dz} \right|_{z \rightarrow 0} = Q^- c_0^- (\ln z + c_1),$$

$$Q^+ \left. \frac{1}{z} \frac{dG}{dz} \right|_{z \rightarrow 0} = Q^+ c_0^+, \quad (8)$$

with the universal coefficients<sup>1,6</sup>

$$Q^- c_0^- \simeq -0.7, \quad Q^+ c_0^+ \simeq 0.9, \quad q = Q^\pm c_\infty^\pm \simeq 0.5. \quad (9)$$

The scaling form (7) with the limits (8), together with the critical exponents (Eq. (3)) and the universal relations (4) and (6) are characteristic properties of the 3D-xy universality class. Accordingly, a homogeneous extreme type II superconductor falls into this universality class when these relations are satisfied. When this is the case the doping dependence of the non-universal critical properties, such as transition temperature  $T_c$ , critical amplitudes of correlation lengths  $\xi_{ab0,c0}^\pm$ , anisotropy  $\gamma$ , *etc.* can be determined, while the universal relations are independent of the doping level.

To determine  $T_c$  we consider the limit  $z \rightarrow \infty$  ( $x \rightarrow 0$ ). Here the scaling form (7) reduces with Eq. (8) to

$$\frac{m}{H^{1/2}} = -\frac{k_B q}{\Phi_0^{3/2}} \gamma T, \quad q = Q^\pm c_\infty^\pm. \quad (10)$$

$Q^+ c_\infty^+ = Q^- c_\infty^-$  follows from the fact that  $m/\sqrt{H_c}$  adopts at the zero-field transition temperature  $T_c$  a unique value where the curves  $m/\sqrt{H}$  *vs.*  $T$  taken at different fields  $H$  cross and  $m/H^{1/2} \gamma T_c$  adopts the universal value

$$\frac{m}{H^{1/2} T_c \gamma} = -\frac{k_B q}{\Phi_0^{3/2}}. \quad (11)$$

Furthermore, at  $T_c$  and in the limit  $H \rightarrow 0$  Eq. (10) also implies

$$\frac{m}{H T_c} = -\frac{k_B q \gamma}{\Phi_0^{3/2}} \frac{1}{H^{1/2}}, \quad (12)$$

describing the divergence of the diamagnetic susceptibility at  $T_c$  when  $H \rightarrow 0$ . Accordingly, the location of a crossing point in  $m/\sqrt{H}$  *vs.*  $T$  provides an estimate for the 3D transition temperature and the factor of proportionality in  $m/(H T_c)$  *vs.*  $H^{1/2}$  probes the anisotropy  $\gamma$ .

Given then  $T_c$  and with that the reduced temperature  $t = T/T_c - 1$ , the dominant fluctuations and their properties can now be explored by invoking the scaling form (7). Considering the plot  $M/(TH^{1/2})$  vs.  $bt$  for various fixed magnetic fields  $H$ , according to Eq. (7) 3D-xy fluctuations are verified when  $b$  scales as  $b \propto H^{1/2\nu}$  with  $\nu \simeq 2/3$ . As  $\text{YBa}_2\text{Cu}_3\text{O}_{7-\delta}$  near optimum doping is concerned, the evidence for this 3D-xy scaling behavior is well established<sup>4,5</sup>. Even though this is an essential step, much more detailed confirmation of 3D-xy universality and the doping dependence of characteristic critical properties can be derived by invoking the limiting forms (8) of the scaling function. Considering the limit  $z \rightarrow 0$ , Eq. (7) reduces below  $T_c$  to

$$\frac{m}{T} = -\frac{Q^- c_0^- k_B}{\Phi_0 \xi_c^-} \left( \ln \left( \frac{H (\xi_{ab}^-)^2}{\Phi_0} \right) + c_1 \right), \quad (13)$$

and above  $T_c$  to

$$\frac{m}{TH} = -\frac{Q^+ c_0^+ k_B (\xi_{ab}^+)^2}{\Phi_0^2 \xi_c^+}. \quad (14)$$

Thus, given the magnetization data of a homogenous system, attaining the limit  $z = H (\xi_{ab0}^\pm)^2 |t|^{-2\nu} / \Phi_0 \ll 1$ , the growth of  $\xi_{ab}$  and  $\xi_c$  is unlimited and estimates for  $\xi_{c0}^-$ ,  $\xi_{ab0}^+$  and  $(\xi_{ab0}^+)^2 / \xi_{c0}^+$  can be deduced from

$$|t|^{-2/3} \frac{m}{T} = -\frac{Q^- c_0^- k_B}{\Phi_0 \xi_{c0}^-} \left( \ln \left( \frac{H (\xi_{ab0}^-)^2}{\Phi_0} \right) + \ln |t|^{-4/3} + c_1 \right) \quad (15)$$

and

$$|t|^{2/3} \frac{m}{TH} = -\frac{Q^+ c_0^+ k_B (\xi_{ab0}^+)^2}{\Phi_0^2 \xi_{c0}^+}, \quad (16)$$

given the values for the universal constants  $Q^- c_0^-$  and  $Q^+ c_0^+$  (Eq. (9)). However, for data taken at fixed magnetic field the reduction of  $z = (H (\xi_{ab0}^\pm)^2 / \Phi_0) |t|^{-4/3}$  unavoidably implies an increasing reduced temperature  $t$  and with that a run away from criticality. Thus, for fixed magnetic field the window where these limiting forms apply is limited to intermediate values of the reduced temperature. Extrinsic limitations arise in the presence of inhomogeneities. In this case the correlation lengths  $\xi_{ab,c}$  cannot grow beyond the lengths  $L_{ab,c}$ , set by the respective extent of the homogenous domains. Indeed, there is the Harris criterion<sup>21</sup>, which states that short-range correlated and uncorrelated disorder is irrelevant at the unperturbed critical point, provided that the specific heat exponent  $\alpha$  is negative. Since in the 3D-XY universality class  $\alpha$  is negative (Eq. (3)), a rounded transition uncovers a finite size effect<sup>22,23</sup>, where the correlation lengths  $\xi_{ab,c} = \xi_{ab0,c0}^+ |t|^{-\nu}$  cannot grow beyond  $L_{ab,c}$ , the respective extent of the homogenous domains. Hence, as long as  $\xi_{ab,c} < L_{ab,c}$  the critical properties of the fictitious homogeneous system can be explored with

the aid of Eqs. (15) and (16). However, closer to  $T_c$  the finite size effect sets in as  $\xi_{ab,c}$  approaches  $L_{ab,c}$ . When  $\xi_c < L_c$  and  $\xi_{ab}$  reaches  $L_{ab}$  a finite size effect appears in the plot  $|t|^{-2/3} m/T$  vs.  $\ln |t|^{-4/3}$  around  $\ln |t_{abp}|^{-4/3}$  ( $\xi_{ab0}^- |t_{abp}|^{-4/3} = L_{ab}$ ) as the onset of deviations from the linear behavior. Even closer to  $T_c$  where both  $\xi_{ab}$  and  $\xi_c$  attain the respective limiting length,  $(m/T)$  tends according to Eq. (13) to diverge as  $f_0 |t|^{-2/3}$  where  $f_0 = -(Q^- c_0^- k_B) / (\Phi_0 L_c) (\ln (H L_{ab}^2 / \Phi_0) + c_1)$ . Accordingly, sufficiently extended magnetization data do not provide estimates for the critical properties of the associated fictitious homogeneous system only, but uncover the extent of the homogenous domains as well. As a unique size of the homogeneous domains is unlikely, the smallest extent will set the scale where the growth of the respective correlation length starts to deviate from the critical behavior of a homogenous system. Hence, the analysis of magnetization data allows to probe the homogeneity of the sample as well, and provides a lower bound for the extent of the homogenous domains. Furthermore, when the outlined analysis of magnetization data uncovers 3D-xy universality, it also implies that the pressure and isotope effects on the critical properties are not independent but related in terms of universal relations such as (4)-(6) and (10). As an example, the universal form (10) implies that the pressure or isotope exchange induced changes of magnetization, transition temperature and anisotropy are related by  $\Delta m(T_c)/m(T_c) = \Delta T_c/T_c + \Delta \gamma(T_c)/\gamma(T_c)$ .<sup>3</sup> Last but not least, it provides estimates for the pressure and isotope effects on the critical amplitudes, the correlation lengths, the transition temperature, the anisotropy and the extent of the homogeneous domains.

We are now prepared to analyze the reversible magnetization data of Salem-Sugui *et al.*<sup>10,11</sup> for underdoped  $\text{YBa}_2\text{Cu}_3\text{O}_{7-\delta}$  single crystals with  $T_c \simeq 41.5$  K and  $T_c \simeq 62$  K. From magnetic torque measurements it is known that in the underdoped regime the chemical substitution tuned reduction of  $T_c$  is accompanied by an increase of the anisotropy. From Fig. 1, showing  $\gamma$  vs.  $T_c$  it is seen that  $\gamma$  increases from 6 around  $T_c \simeq 91$  K to 29 near  $T_c \simeq 40$  K.

It is well documented that in highly anisotropic cuprate superconductors the magnetization curves  $M(T)$  taken at varying fields cross below  $T_c$  around  $(T_{\text{cross}}, M_{\text{cross}})$ , nearly independent of the magnitude of the applied field<sup>24</sup>. Although this crossing phenomenon is not associated with criticality, it uncovers that the system behaves below  $T_{\text{cross}}$  nearly quasi two dimensional<sup>1,24,25</sup>. In Fig. 2 we depicted the data of Salem-Sugui *et al.*<sup>10,11</sup> for underdoped  $\text{YBa}_2\text{Cu}_3\text{O}_{7-\delta}$  single crystals with  $T_c \simeq 41.5$  K and  $T_c \simeq 62$  K in terms of  $M$  vs.  $T$  for varying  $H$  applied along the  $c$ -axis. Apparently there are nearly field independent crossing points around  $T_{\text{cross}} \simeq 40.3$  K and 60.5 K. This phenomenon is however absent in nearly optimally doped and with that considerably less anisotropic

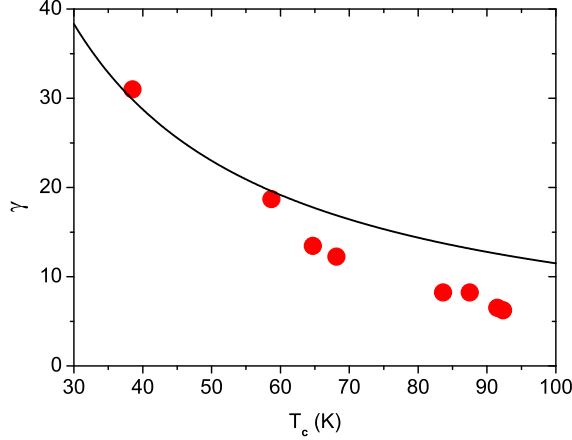


FIG. 1:  $\gamma$  vs.  $T_c$  for  $\text{YBa}_2\text{Cu}_3\text{O}_{7-\delta}$  derived from Janossy *et al.*<sup>13</sup> To estimate  $\gamma$  for the  $T_c$ 's considered here we use  $\gamma = 1150/T_c$  indicated by the solid line.

$\text{YBa}_2\text{Cu}_3\text{O}_{7-\delta}$  samples.<sup>24</sup> Since  $\gamma$  increases with reduced  $T_c$  (see Fig. 1), the occurrence of a nearly field independent crossing point uncovers then a 3D to quasi 2D crossover below  $T_{\text{cross}}$ .

Nevertheless, above  $T_{\text{cross}}$  3D-xy fluctuations are expected to set in and to dominate. In this case Eq. (10) implies the occurrence of a crossing point in  $M/(TH^{1/2})$  vs.  $T$  at  $T_c$ . The plots shown in Fig. 3 uncover these crossing points and provide for the respective transition temperatures the estimates  $T_c \simeq 41.5$  K and  $T_c \simeq 62$  K.

To identify the dominant fluctuations we replotted the data depicted in Fig. 4a in terms of  $M/(TH^{1/2})$  vs.  $bt$  with  $b$  adjusted to achieve a collapse on the  $H = 0.1$  T curve close to  $t = 0$ . According to Eq. (7) the dominance of 3D-xy fluctuations is established when  $b$  scales as  $b \propto 1/H^{1/2\nu} \propto 1/H^{3/4}$ . In Fig. 4b, depicting the field dependence of  $b$ , we observe remarkable consistency with the characteristic 3D-xy behavior. However, the quality of the data collapse is seen to deteriorate with increasing field.

According to Fig. 5, showing the corresponding plots for the sample with  $T_c \simeq 62$  K, we observe again consistency with the characteristic 3D-xy critical behavior,  $b \simeq H^{-3/4}$ . Even though the data collapse is seen to deteriorate with increasing field as well, these plots uncover the dominance of 3D-xy fluctuations around the estimated transition temperature  $T_c$ .

Having established the consistency with 3D-xy universality in terms of scaling plots based on the universal scaling form (7) with  $\nu \simeq 2/3$  and the estimates for  $T_c$  we are no prepared to perform a more detailed analysis providing additional checks, allowing to explore the inhomogeneity induced finite size effects and to estimate the essential critical properties, including the critical amplitudes of the correlation lengths and the anisotropy. The basic starting point is either the limiting behavior below or above  $T_c$ , given by Eqs.(15) and (16), respectively.

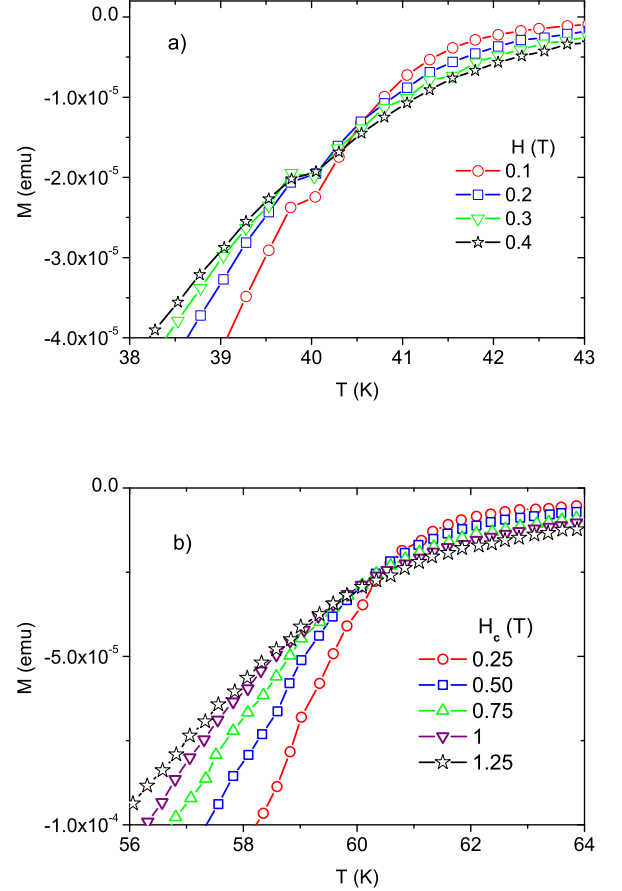


FIG. 2: Reversible magnetization  $M$  vs.  $T$  for various fixed magnetic fields  $H$  applied along the  $c$ -axis of underdoped  $\text{YBa}_2\text{Cu}_3\text{O}_{7-\delta}$  single crystals with  $T_c \simeq 41.5$  K (a) and  $T_c \simeq 62$  K (b) derived from the data of Salem-Sugui *et al.*<sup>10,11</sup> There are nearly field independent crossing points around  $T_{\text{cross}} \simeq 40.3$  K and 60.5 K.

TABLE I:  $T_c$ , weight of the samples and relationship between  $M$  in emu and  $m = M\rho/\text{weight}$  with  $\rho \simeq 6.3$  g/cm<sup>3</sup>.

$T_c$ (K)	weight (mg)	$m$ (emu cm <sup>-3</sup> )
41.5	1	6300 $M$
62	1.2	5250 $M$

To invoke these limiting forms it is necessary to convert the magnetization data given in emu to m in emu cm<sup>-3</sup> according to Table I.

Next we invoke the limiting form Eq. (15) to estimate the magnitude of the critical amplitudes below  $T_c$  and to explore the homogeneity of the samples. For this purpose we depicted in Fig. 6  $|t|^{-2/3} m/T$  vs.  $\ln |t|^{-4/3}$ . In both samples we observe in a limited interval consistency with the asymptotic behavior, indicated by the straight lines. Using Eqs. (9) and (15) we derive from the slope of these

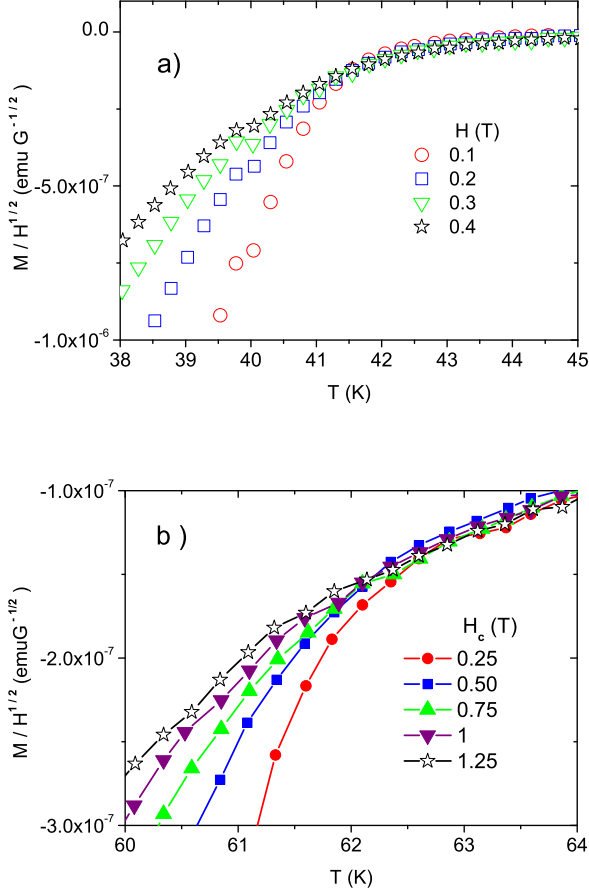


FIG. 3:  $M/H^{1/2}$  vs.  $T$  at various fixed magnetic fields  $H$  applied along the  $c$ -axis of underdoped  $\text{YBa}_2\text{Cu}_3\text{O}_{7-\delta}$  single crystals with  $T_c \simeq 41.5$  K (a) and  $T_c \simeq 62$  K (b) derived from the data of Salem-Sugui *et al.*<sup>10,11</sup> The crossing points provide an estimate for the respective transition temperature,  $T_c \simeq 41.5$  K (a) and  $T_c \simeq 62$  K (b)

lines the estimates

$$\xi_{c0}^- \simeq 1.46 \text{ \AA} \quad (T_c \simeq 41.5 \text{ K}), \quad \xi_{c0}^- \simeq 1.33 \text{ \AA} \quad (T_c \simeq 62 \text{ K}), \quad (17)$$

for the critical amplitude of the  $c$ -axis correlation length.

From the straight lines in Fig. 6 it also follows that

$$\ln \frac{10^3 (\xi_{ab0}^-)^2}{\Phi_0} = -5.09 - c_1 \quad (T_c \simeq 41.5 \text{ K}),$$

$$\ln \frac{2.5 \cdot 10^3 (\xi_{ab0}^-)^2}{\Phi_0} = -5.39 - c_1 \quad (T_c \simeq 62 \text{ K}), \quad (18)$$

yielding for the critical amplitudes of the in-plane correlation lengths the ratio

$$\frac{\xi_{ab0}^- (T_c \simeq 41.5 \text{ K})}{\xi_{ab0}^- (T_c \simeq 62 \text{ K})} \simeq 1.54. \quad (19)$$

In addition, this plot reveals that the attainable critical regime, indicated by the straight lines, ends around

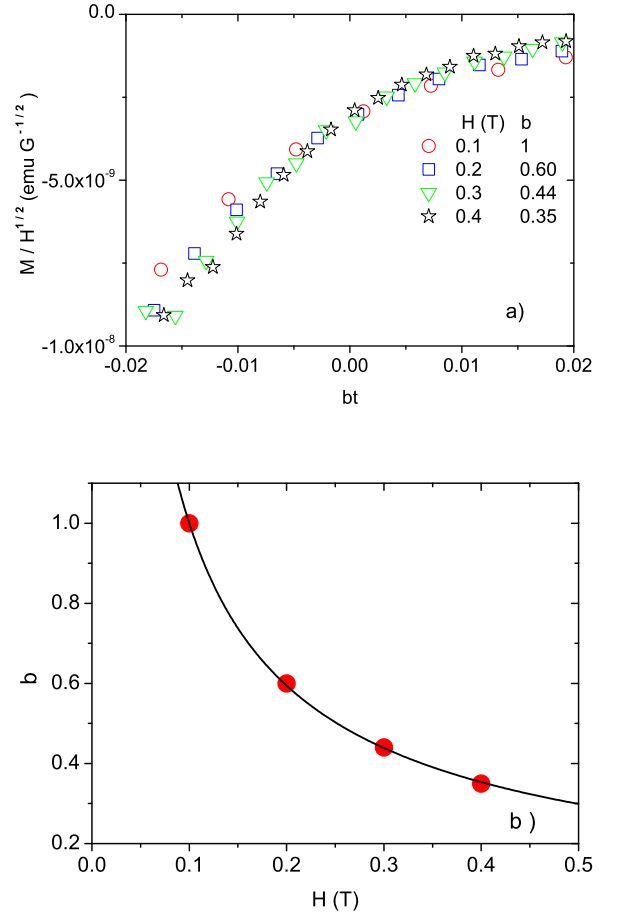


FIG. 4: a)  $M/(TH^{1/2})$  vs.  $bt$  with  $b$  adjusted to achieve a collapse on the  $H = 0.1$  T curve for the data shown in Fig. 3a. b)  $b$  vs.  $H$ . The solid line is  $b \propto H^{-3/4}$  characteristic for 3D-xy thermal fluctuations.

the marked values  $\ln |t_{abp}|^{-4/3} \simeq 4.12$  and  $\ln |t_{abp}|^{-4/3} \simeq 4.46$ . Here the in-plane correlation length  $\xi_{ab}$  reaches the limiting length  $L_{ab}$ , so that  $\xi_{ab0}^- |t_{abp}|^{-2/3} = L_{ab}$ . From  $\ln |t_{abp}|^{-4/3} \simeq 4.12$  and  $\ln |t_{abp}|^{-4/3} \simeq 4.46$  and Eq. (19) we obtain for the ratio between the limiting lengths  $L_{ab}$  the estimate

$$\frac{L_{ab} (T_c \simeq 41.5 \text{ K})}{L_{ab} (T_c \simeq 62 \text{ K})} \simeq 1.36. \quad (20)$$

Nevertheless, given the estimate for the universal coefficient  $c_1$ , we can extract from Eq. (18) the critical amplitude of the in-plane correlation length of the respective fictitious homogeneous system. Using  $c_1 = 1.76$ , which will be derived later on, we obtain

$$\xi_{ab0}^- \simeq 46.82 \text{ \AA} : T_c \simeq 41.5 \text{ K}, \quad \xi_{ab0}^- \simeq 27.32 \text{ \AA} : T_c \simeq 62 \text{ K} \quad (21)$$

and together with the values for  $\xi_{c0}^-$  (Eq. (17)) for the anisotropy

$$\gamma \simeq 32.07 : T_c \simeq 41.5 \text{ K}, \quad \gamma \simeq 20.5 : T_c \simeq 62 \text{ K}, \quad (22)$$



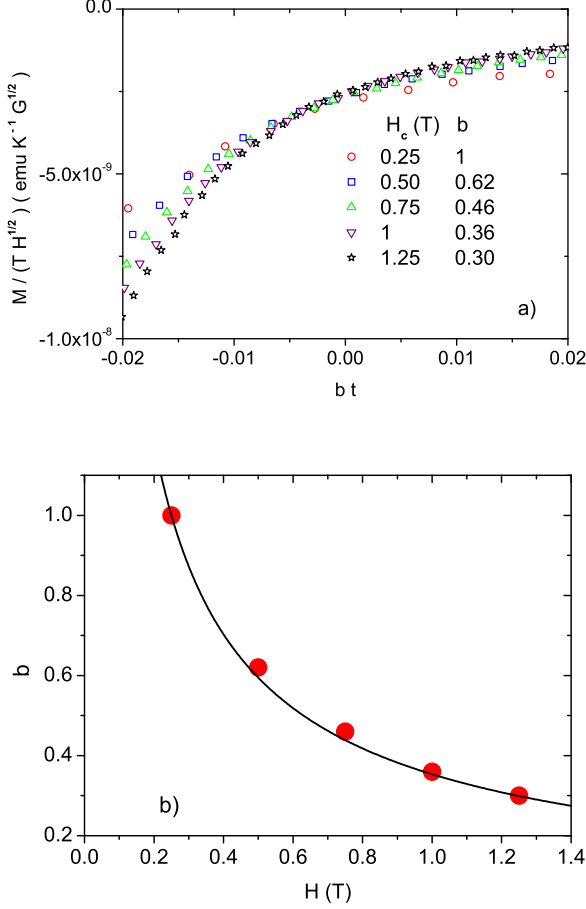


FIG. 5: a)  $M/(TH^{1/2})$  vs.  $bt$  with  $b$  adjusted to achieve a collapse on the  $H = 0.25$  T curve for the data shown in Fig. 3b. b)  $b$  vs.  $H$ . The solid line is  $b \propto H^{-3/4}$  characteristic for 3D-xy thermal fluctuations.

in reasonable agreement with the estimates derived from the magnetic torque measurements, namely  $\gamma \simeq 28$  and  $19$  (see Fig. 1).

To analyze the behavior closer to  $T_c$  we consider the plot  $-|t|^{-2/3} m/T$  vs.  $-t$  shown in Fig. 7. Above  $t_{abp} \simeq 0.046$  (Fig. 7a) and  $t_{abp} \simeq 0.034$  (Fig. 7b) there is an interval exhibiting the  $\ln|t|^{-4/3}$  behavior of a homogeneous system, indicated by the solid curve and consistent with the  $|t|^{-2/3} m/T$  vs.  $\ln|t|^{-4/3}$  plots shown in Fig. 6. Indeed, a minimum occurs below  $t_{abp}$  followed by an increase. Although the data is sparse, it indicates a  $|t|^{-2/3}$  divergence, associated with a finite size effect in both,  $\xi_{ab}$  and  $\xi_c$ , whereby these correlation lengths cannot grow beyond  $L_{ab}$  and  $L_c$ , respectively. According to Eq. (15) the amplitude of the divergence is given by

$$\begin{aligned} |t|^{-2/3} \frac{m}{T} &= -\frac{Q^- c_0^- k_B}{\Phi_0 L_c} \left( \ln \left( \frac{H L_{ab}^2}{\Phi_0} \right) + c_1 \right) |t|^{-2/3} \\ &= f_0 |t|^{-2/3}, \end{aligned} \quad (23)$$

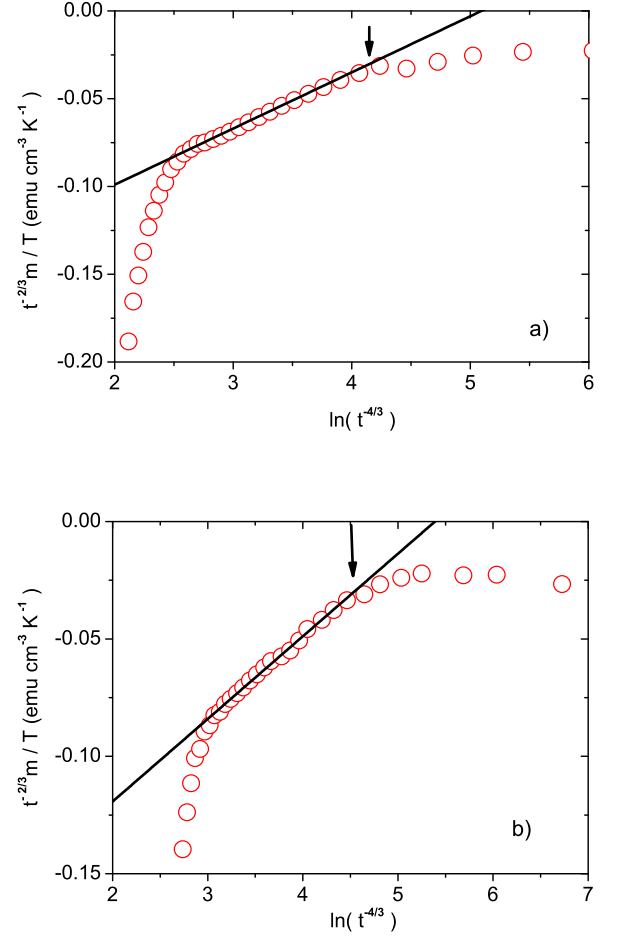


FIG. 6:  $|t|^{-2/3} m/T$  vs.  $\ln|t|^{-4/3}$  for  $t < 0$ . a) Sample with  $T_c \simeq 41.5$  K at  $H = 0.1$  T; the solid line is  $|t|^{-2/3} m/T = -0.163 + 0.032 \ln|t|^{-4/3}$ . The arrow marks  $\ln|t_{abp}|^{-4/3} \simeq 4.12$  ( $t_{abp} \simeq -0.045$ ). b) Sample with  $T_c \simeq 62$  K at  $H = 0.25$  T; the solid line is  $|t|^{-2/3} m/T = -0.189 + 0.035 \ln|t|^{-4/3}$ . The arrow marks  $\ln|t_{abp}|^{-4/3} \simeq 4.46$  ( $t_{abp} \simeq -0.035$ ).

and allows to determine  $L_c$ , given the amplitude  $f_0$ ,  $L_{ab}$  and  $c_1$ . From  $\ln|t_{abp}|^{-4/3} \simeq 4.12$  (Fig. 6a),  $\xi_{ab0}^- \simeq 46.82$  Å (Eq. (21)) and  $\ln|t_{abp}|^{-4/3} \simeq 4.46$ ,  $\xi_{ab0}^- \simeq 27.32$  Å we obtain with  $\xi_{ab}(t_{abp}) = \xi_{ab}^- |t_{abp}|^{-2/3} = L_{ab}$  for the limiting length in the  $ab$ -plane the estimate,

$$L_{ab} \simeq 367 \text{ Å}; T_c \simeq 41.5 \text{ K}, L_{ab} \simeq 254 \text{ Å}; T_c \simeq 62 \text{ K}, \quad (24)$$

in reasonable agreement with the estimate for their ratio given by Eq. (20). Together with  $Q^- c_0^- \simeq -0.7$  (Eq. (9)),  $c_1 = 1.76$  and the rather crude estimates for  $f_0$  (see Fig. (7)) Eq. (23) yields

$$L_c \simeq 57 \text{ Å}; T_c \simeq 41.5 \text{ K}, L_c \simeq 53 \text{ Å}; T_c \simeq 62 \text{ K}, \quad (25)$$

in comparison with the previous estimates,  $L_{ab} \simeq 392$  Å and  $L_c \simeq 52$  Å for  $\text{YBa}_2\text{Cu}_3\text{O}_{6.7}$  with  $T_c \simeq 59.7$  K, derived from the inhomogeneity induced finite size effect in

the temperature dependence of the in-plane penetration depth close to criticality.<sup>27</sup>

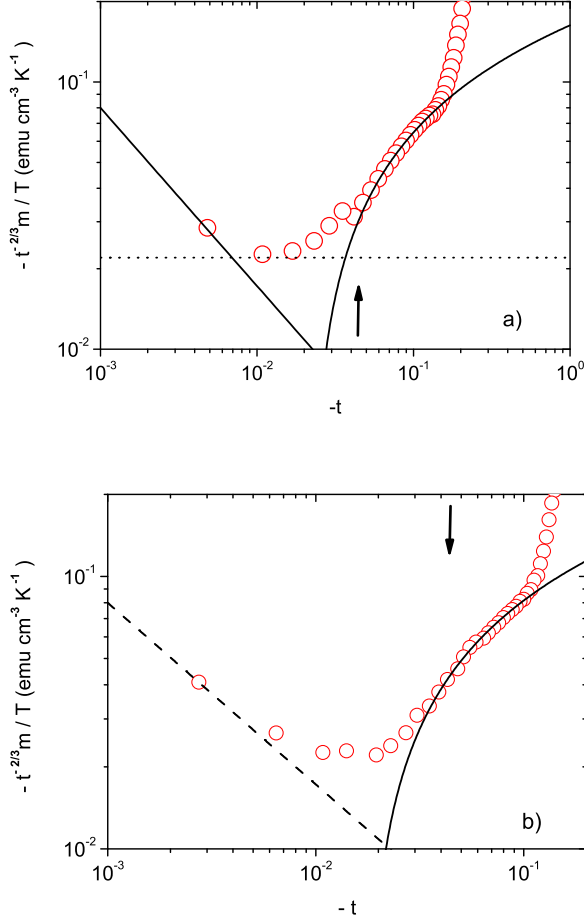


FIG. 7:  $-|t|^{-2/3} m/T$  vs.  $-t$  for  $t < 0$ . a) Sample with  $T_c \simeq 41.5$  K at  $H = 0.1$  T; the solid curve is  $-|t|^{-2/3} m/T = 0.15 - 0.03 \ln |t|^{-4/3}$  and the dashed one  $-|t|^{-2/3} m/T = 8 \cdot 10^{-4} |t|^{-2/3}$ . The arrow marks  $t_{abp} \simeq -0.047$  ( $\ln |t_{abp}|^{-4/3} \simeq 4.12$ ). b) Sample with  $T_c \simeq 62$  K at  $H = 0.25$  T; the solid line is  $-|t|^{-2/3} m/T = 0.19 - 0.035 \ln |t|^{-4/3}$  and the dashed one  $-|t|^{-2/3} m/T = 0.0008 |t|^{-2/3}$ . The arrow marks  $t_{abp} \simeq -0.042$  ( $\ln |t_{abp}|^{-4/3} \simeq 4.46$ ).

Further estimates of the critical amplitudes of the correlation and limiting lengths can be obtained by invoking Eq. (14). According to this we plotted  $|t|^{2/3} m/(TH)$  vs.  $t$  for the sample with  $T_c \simeq 41.5$  K and  $H = 0.2$  T in Fig. 8a. As  $t$  tends to zero the data approaches a minimum around  $t = t_{cp} \simeq 0.026$ , indicated by the horizontal line and marked by the arrow. This minimum provides an estimate for the critical behavior given by Eq. (14), while the upturn below uncovers again an inhomogeneity induced limiting length along the  $c$ -axis and in the  $ab$ -plane. Indeed, when the growth of  $\xi_{ab,c}$  are limited by  $L_{ab,c}$ ,  $|t|^{2/3} m/(TH)$  tends to zero because the ratio  $\xi_{ab}^2/\xi_c$  approaches the ratio  $L_{ab}^2/L_c$ . A glance to Fig. 8b reveals that the minimum exhibits a linear field dependence.

Accordingly, the limiting behavior  $dG/dz = c_0^+ z$  (Eq. (8)) is not attained and the lowest magnetic field dependent correction, compatible with the linear dependence,  $dG/dz = c_0^+ z(1 + gz)$ , must be taken into account. The linear extrapolation yields

$$\frac{Q^+ c_0^+ k_B (\xi_{ab0}^+)^2}{\Phi_0^2 \xi_{c0}^+} = 2.08 \cdot 10^{-8} \text{ (emu cm}^{-3} \text{K}^{-1} \text{G}^{-1}), \quad (26)$$

and with the universal coefficient  $Q^+ c_0^+ \simeq 0.9$  (Eqs.(9))

$$(\xi_{ab0}^+)^2 / \xi_{c0}^+ = \gamma \xi_{ab0}^+ \simeq 718 \text{ \AA}. \quad (27)$$

Invoking then our estimate for the anisotropy,  $\gamma \simeq 32.07$  (Eq. (22)) we obtain

$$\xi_{ab0}^+ \simeq 22.4 \text{ \AA}, \quad \xi_{c0}^+ = \xi_{ab0}^+ / \gamma \simeq 0.7 \text{ \AA}, \quad (28)$$

and with  $\xi_{c0}^- \simeq 1.46 \text{ \AA}$  (Eq. (19)) for the universal ratio

$$\frac{\xi_{c0}^-}{\xi_{c0}^+} = \frac{\xi_{ab0}^-}{\xi_{ab0}^+} \simeq 2.1, \quad (29)$$

compared to the theoretical prediction  $\xi_{c0}^-/\xi_{c0}^+ = \xi_{ab0}^-/\xi_{ab0}^+ \simeq 2.21$  (Eq. (4)). Unfortunately, an equivalent analysis of the data for the less underdoped sample with  $T_c \simeq 62$  K is not opportune, because the measurements do not extend to comparably low fields.

In Table II we summarized our estimates for the critical properties of underdoped  $\text{YBa}_2\text{Cu}_3\text{O}_{7-\delta}$  single crystals derived from the magnetization data of Salem-Sugui *et al.*<sup>10,11</sup>. For comparison we included corresponding values for nearly optimally doped  $\text{YBa}_2\text{Cu}_3\text{O}_{7-\delta}$ <sup>17</sup>. While the critical amplitude of the  $c$ -axis correlation length  $\xi_{c0}^\pm$  exhibits a rather weak doping dependence the  $ab$ -plane counterpart,  $\xi_{ab0}^\pm$ , and the anisotropy increase drastically with reduced  $T_c$ . As a consequence, the correlation volume  $V_{corr}^- = (\xi_{ab0}^-)^2 \xi_{c0}^-$  increases and the critical amplitude of the specific heat singularity  $A^-$  (Eq. (5)) decreases dramatically. This behavior renders it difficult to extract in the underdoped regime critical behavior from specific heat data. Because  $\xi_{c0}^-$  does not change much with reduced  $T_c$ , the critical amplitude of the in-plane correlation length  $\lambda_{ab0}$ , resulting from Eq. (11), rises considerably, reflecting the behavior of its zero temperature counterpart  $\lambda_{ab}(0)$ , where  $\lambda_{ab}(0) \simeq 1300 \text{ \AA}$  and  $\lambda_{ab}(0) \simeq 2250 \text{ \AA}$  at  $T_c = 91.3$  K and 60.5 K, respectively<sup>12</sup>. Conversely, although both, the critical amplitudes of the in-plane correlation length  $\xi_{ab0}^-$  and penetration depth  $\lambda_{ab0}$  increase with reduced  $T_c$ , the ratio  $\lambda_{ab0}/\xi_{ab0}^-$ , corresponding to the Ginzburg-Landau parameter  $\kappa_{ab}$ , decreases substantially, whereupon  $\text{YBa}_2\text{Cu}_3\text{O}_{7-\delta}$  crosses over from an extreme to a weak type-II superconductor. Noting again that the size of the homogeneous domains is not necessarily unique, the onset of the finite size effect probes their respective smallest extent. Accordingly our estimates for  $L_{ab}$  and  $L_c$  are lower bounds for the extent of the homogenous domains.

TABLE II: Collection of the estimates derived from the magnetization data of Salem-Sugui *et al.*<sup>10,11</sup> for the underdoped YBa<sub>2</sub>Cu<sub>3</sub>O<sub>7- $\delta$</sub>  single crystals. For comparison we included the estimates for nearly optimally doped YBa<sub>2</sub>Cu<sub>3</sub>O<sub>7- $\delta$</sub> .<sup>17</sup> The bracketed values for  $\xi_{c0}^+$  and  $\xi_{ab0}^+$  are obtained with Eq. (4).  $V_{corr}^- = (\xi_{ab0}^-)^2 \xi_{c0}^-$  denotes the correlation length volume below  $T_c$ . To obtain the critical amplitude of the magnetic in-plane penetration depths  $\lambda_{ab0}$  we used the universal relation (6).

$T_c$ K	$\xi_{c0}^-$ Å	$\xi_{ab0}^-$ Å	$\gamma = \xi_{ab0}^-/\xi_{c0}^-$	$\xi_{c0}^+$ Å	$(\xi_{ab0}^+)^2/\xi_{c0}^+$ Å	$\xi_{ab0}^+$ Å	$V_c^-$ Å <sup>3</sup>	$L_{ab}$ Å	$L_c$ Å	$10^{-3}\lambda_{ab0}$ Å	$\lambda_{ab0}/\xi_{ab0}^-$	$10^{-6}\lambda_{ab0}^2 T_c$ Å <sup>2</sup> K
91.7	1.3	10	8	-	-	-	130	-	-	0.941	90	81.2
62	1.33	27.32	20.5	(0.60)	-	(12.36)	993	254	53	1.157	42	83.0
41.5	1.46	46.82	32.07	0.70	718	22.4	3200	367	57	1.482	32	91.1

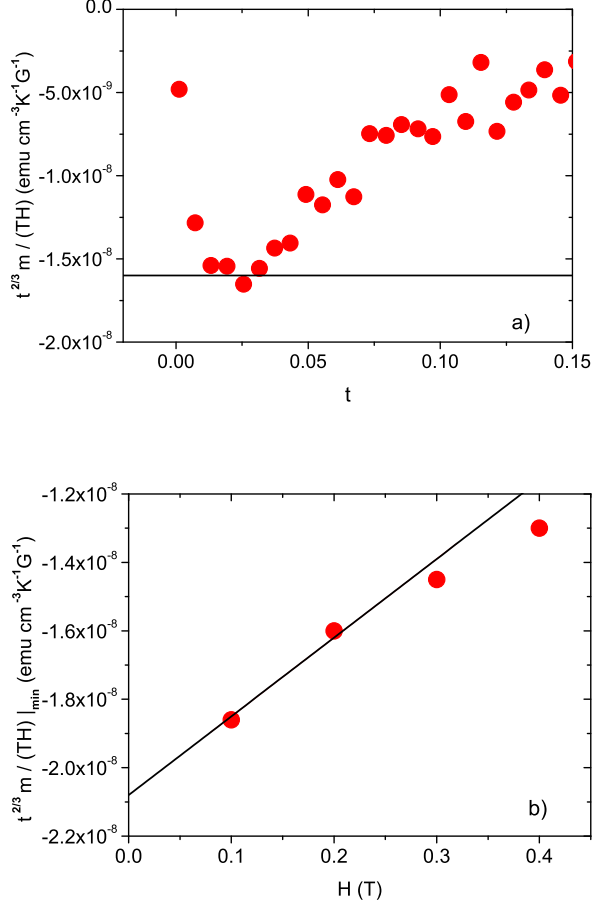


FIG. 8: a)  $|t|^{2/3} m / (TH)$  vs.  $t$  for the sample with  $T_c \simeq 41.5$  K and  $H = 0.2$  T. The horizontal line marks the minimum. b)  $|t|^{2/3} m / (TH) |_{\min}$  vs.  $H$  for the sample with  $T_c \simeq 62$  K and  $H = 0.25$  T. The line is  $|t|^{2/3} m / (TH) |_{\min} = -2.08 \cdot 10^{-8} + 2.3 \cdot 10^{-8} H$  with  $H$  in T.

In this context it is important to recognize that the listed anisotropies refer to the homogeneous counterparts. However, in the actual inhomogeneous samples these values only apply in an intermediate temperature regime where the growth of the correlation length is not yet limited by the finite size effect. Indeed, considering the sample with  $T_c = 41.5$  K, below  $T_c$   $\xi_{ab}$  levels off around  $|t_{abp}| \simeq 0.045$ , while  $\xi_c$  saturates around

$|t_{cp}| \simeq 0.0041$ . Accordingly, below  $|t_{abp}|$  the anisotropy  $\gamma = \xi_{ab}/\xi_c$  decreases from  $\gamma = \xi_{ab0}^-/\xi_{c0}^- \simeq 32$  to  $\gamma = L_{ab}/L_c \simeq 6.4$  at  $T_c$ . This behavior implies that the 2D-limit in the underdoped regime is hardly accessible because  $\xi_{ab}$  cannot grow beyond  $L_{ab}$  and as a result  $\gamma$  does not diverge for fixed  $\xi_c$ .

To check the consistency of our analysis further, we invoke Eq. (5) to calculate from the magnetization data the derivative of the universal scaling function in terms of

$$Q^\pm \frac{dG}{dz} = -\frac{m}{T} \frac{\Phi_0}{k_B} \xi_{c0}^\pm |t|^{-2/3}, \quad z = \left( H (\xi_{ab0}^\pm)^2 / \Phi_0 \right) |t|^{-4/3}, \quad (30)$$

and the respective estimates for the critical amplitudes of the correlation lengths (Table II). In Fig. 9a, showing  $-Q^- dG/dz$  vs.  $\ln(z)$  below  $T_c$ , we observe from  $\ln(z) \simeq -2.75$  down to  $-4.25$  consistency with the leading  $z \rightarrow 0$  behavior  $Q^- dG/dz = Q^- c_0^- (\ln(z) + c_1)$ , where  $Q^- c_0^- = -0.7$  (Eq. (9)) and  $c_1$  was chosen as

$$c_1 = 1.76. \quad (31)$$

This estimate fixes the so far unknown universal coefficient  $c_1$ . The systematic deviations, setting in around  $\ln(z) \simeq -2.75$  ( $z \simeq 0.065$ ), uncover the onset of the inhomogeneity induced finite size effect, limiting the growth of  $\xi_{ab}$ . Indeed, this value corresponds to  $z = H L_{ab}^2 / \Phi_0$  with  $H = 0.1$  T and  $L_{ab} = 367$  Å (Table II). On the other hand, the upturn setting in around  $\ln(z) \simeq -4.2$  ( $z \simeq 0.0136$ ) signals the escape from the scaling regime where the  $\ln(z)$  behavior applies. Indeed, in the present case  $H$  is fixed and the reduction of  $z = \left( H (\xi_{ab0}^+)^2 / \Phi_0 \right) |t|^{-4/3}$  unavoidably implies an increasing reduced temperature  $t$  and with that a run away from criticality. Thus, for fixed magnetic field the window where the universal scaling function can be observed is limited from below by the run away from criticality and from above by the finite size effect in  $\xi_{ab}$ . In Fig. 9b we depicted  $Q^+ d^2 G / dz^2 = -d \left( m \xi_{c0}^- |t|^{-2/3} \Phi_0 / (k_B T) \right) / dz$  vs.  $z = \left( H (\xi_{ab0}^+)^2 / \Phi_0 \right) |t|^{-4/3}$ . According to Eq. (9) it approaches in a homogenous system in the limit  $z \rightarrow 0$  the universal value  $Q^+ d^2 G / dz^2 = Q^+ c_0^+ \simeq 0.9$ . Even though the available data are rather sparse we observe in the interval  $0.01 \lesssim z \lesssim 0.04$  consistency with this



limiting behavior, indicated by the horizontal line. Unfortunately, the available data do not allow to locate the onset of the finite size effect in  $\xi_{ab}$ , seen below  $T_c$  around  $\ln(z) = \ln(HL_{ab}^2/\Phi_0) \simeq \ln(0.065) \simeq -2.73$  (Fig. 9a). The upturn setting in around  $z = 0.01$  signals the run-away from criticality as in Fig. 9a.

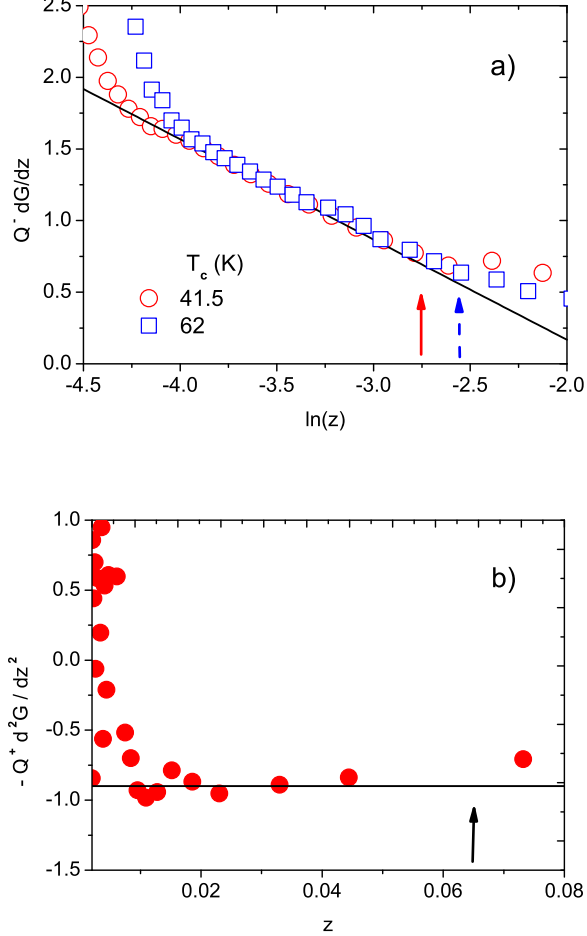


FIG. 9: a)  $Q^- dG/dz = -(m\Phi_0/Tk_B)\xi_{c0}^-|t|^{-2/3}$  vs.  $\ln(z)$  for the sample with  $T_c = 41.5$  K at  $H = 0.1$  T,  $\xi_{ab0}^- = 46.82$  Å and  $\xi_{c0}^- = 1.46$  Å (○) and the sample with  $T_c = 62$  K at  $H = 0.25$  T,  $\xi_{ab0}^- = 27.32$  Å and  $\xi_{c0}^- = 1.33$  Å (□); the solid line is  $Q^- dG/dz = Q^- c_0^- (\ln(z) + c_1)$  with  $z = (H(\xi_{ab0}^-)^2/\Phi_0)|t|^{-4/3}$ ,  $Q^- c_0^- = -0.7$  (Eq. (9)), and  $c_1 = 1.76$  (Eq. (31)). The arrows mark the onset of the finite size effect in  $\xi_{ab}$  at  $\ln(z) = HL_{ab}^2/\Phi_0$ , namely  $\ln(z) = -2.73$  ( $T_c = 41.5$  K) and  $\ln(z) = -2.55$  ( $T_c = 62$  K). b)  $Q^+ d^2G/dz^2 = -d(m(\Phi_0/Tk_B)\xi_{c0}^+|t|^{-2/3})/dz$  vs.  $z = (H(\xi_{ab0}^+)^2/\Phi_0)|t|^{-4/3}$  with  $T_c = 41.5$  K for  $\xi_{ab0}^+ = 22.4$  Å and  $\xi_{c0}^+ = 0.7$  Å; the solid line is  $Q^+ d^2G/dz^2 = Q^+ c_0^+$  with  $Q^+ c_0^+ \simeq 0.9$  (Eq. (9)). The arrow marks  $z = HL_{ab}^2/\Phi_0 \simeq 0.065$ , the onset of the finite size effect in  $\xi_{ab}$ .

Next we turn to magnetization data of Babić *et al.*<sup>5</sup>, taken at fixed temperatures below  $T_c$  as a function of the magnetic field applied along the  $c$ -axis. Here we analyze

the data of the  $\text{YBa}_2\text{Cu}_3\text{O}_{7-\delta}$  single crystal with  $T_c \simeq 93.5$  K. In Fig. 10 we show  $M$  vs.  $\ln(H)$ . In a limited interval we observe linear behavior so that the scaling form (13) rewritten in the form

$$M = -\frac{VQ^-c_0^-k_BT}{\Phi_0\xi_c} \left( \ln(H) + \ln\left(\frac{\xi_{ab}^2}{\Phi_0}\right) + c_1 \right) = d + e \ln(H), \quad (32)$$

applies. The solid lines are this scaling form with the parameters  $d$  and  $e$  listed in Table III.

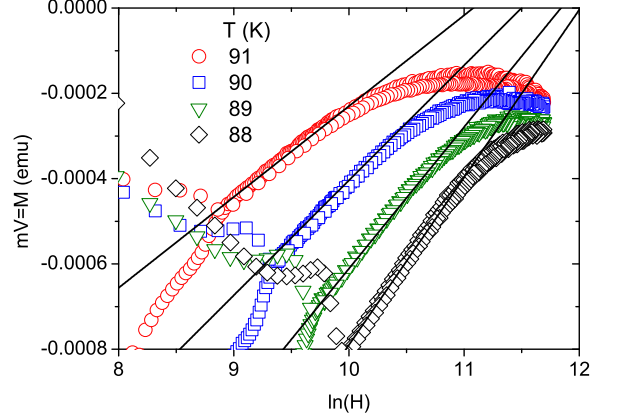


FIG. 10:  $M$  vs.  $\ln(H)$  for various temperatures derived from the data of Babić *et al.*<sup>5</sup> for a  $\text{YBa}_2\text{Cu}_3\text{O}_{7-\delta}$  single crystal with  $T_c \simeq 93.5$  K and the magnetic field applied along the  $c$ -axis. The solid lines are Eq. (32) with the parameters listed in Table III

Given the volume of the sample, the universal amplitudes  $Q^-c_0^- \simeq -0.9$  (Eq. (9)) and  $c_1$  (Eq. (31)) the listed correlation lengths are then readily calculated. Together with  $\xi_{ab,c} = \xi_{ab0,c0}^-|t|^{-2/3}$  we obtain for the critical amplitudes the estimates

$$\xi_{ab0}^- \simeq 7 \text{ Å}, \quad \xi_{c0}^- \simeq 1.4 \text{ Å}, \quad (33)$$

in comparison with  $\xi_{ab0}^- \simeq 10.4$  Å and  $\xi_{c0}^- \simeq 1.3$  Å for the sample with  $T_c = 91.7$  K (Table II).

TABLE III: Parameters entering Eq. (32), yielding the straight lines in Fig. 11 and with  $Q^-c_0^- = -0.7$  (Eq. (9)),  $c_1 = 1.76$  (Eq. (31)) and  $V = 8.2 \cdot 10^{-4} \text{ cm}^{-3}$ <sup>5</sup> the estimates for the correlation lengths  $\xi_{ab}$  and  $\xi_c$ .

$T(\text{K})$	$d$ (emu)	$e$ (emu)	$\xi_{ab}(\text{Å})$	$\xi_c(\text{Å})$
91	$-2.36 \cdot 10^{-3}$	$2.13 \cdot 10^{-4}$	74.1	16.3
90	$-3.10 \cdot 10^{-3}$	$2.70 \cdot 10^{-4}$	59.5	12.8
89	$-3.93 \cdot 10^{-3}$	$3.32 \cdot 10^{-4}$	50.7	10.3
88	$-4.72 \cdot 10^{-3}$	$3.93 \cdot 10^{-4}$	46.5	8.8

To check the consistency with the scaling form (32) further, we calculated  $m\Phi_0\xi_c/(k_BT) = -Q^-dG/dz$  vs.  $z$  for  $T = 91$  K and 90 K as shown in Fig. 11

with the parameters listed in Table III. The comparison with the leading  $z \rightarrow 0$  behavior,  $-Q^- dG/dz = -Q^- c_0^- (\ln(z + c_1))$ , reveals that this regime is attained, but limited by irreversibility in the limit  $z \rightarrow 0$  and the crossover to the large  $z$ -limit,  $-Q^- dG/dz = -qz^{1/2}$  with  $q \simeq 0.5$  (Eq. (9)). This limitation is also apparent in Fig. 10 on the low and high field side. Indeed, because the data do not extend close to  $T_c$ , the correlation lengths are comparatively small and their growths is not yet limited by the extent of the homogenous domains.

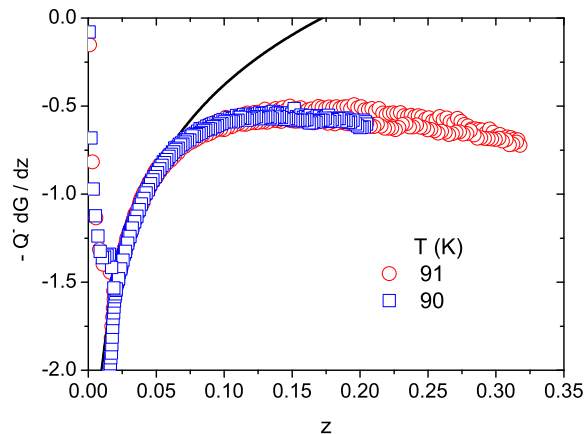


FIG. 11:  $m\Phi_0\xi_c/(k_B T) = -Q^- dG/dz$  vs.  $z$  for  $T = 91$  K and  $90$  K. The solid line is  $-Q^- dG/dz = -Q^- c_0^- (\ln(z + c_1))$  with  $Q^- c_0^- = -0.7$  (Eq. (9)),  $c_1 = 1.76$  (Eq. (31)).

Although the analyzed magnetization data is afflicted with uncertainties arising from the subtraction of the normal state paramagnetism and the Curie term due to paramagnetic impurities or defects, we observed remarkable consistency with 3D-xy critical behavior for both, nearly optimally doped and underdoped samples. In contrast to previous work<sup>4,5</sup> we did not establish the consistency with the 3D-xy scaling plots only, but estimated, given the critical exponent of the correlation lengths,  $\nu \simeq 2/3$ , the critical amplitudes of the correlation length, the universal ratios, etc., of the associated fictitious homogeneous system as well. Indeed, the universality class to which a given experimental sys-

tem belongs is not only characterized by its critical exponents but also by various critical point amplitude ratios and universal coefficients. This has been achieved by invoking the limiting behavior of the universal scaling function  $dG/dz$ , allowing via Eqs. (13)-(16) to explore the growth of the in-plane and  $c$ -axis correlation lengths as  $T_c$  is approached from below or above. We have seen that this growth is limited due to inhomogeneities and that this limitation appears to be equivalent to a finite size effect, whereupon the correlation lengths cannot grow beyond the extent of the homogeneous domains. Clearly, such an analysis does not discriminate between intrinsic or extrinsic inhomogeneities, but it provides lower bounds for the extent of the homogeneous domains seen by the relevant fluctuations. Even though since the discovery of superconductivity in the cuprates by Bednorz and Müller<sup>28</sup> a tremendous amount of work has been devoted to their characterization, the issue of inhomogeneities and their characterization is still a controversial issue. There is neutron spectroscopic evidence for nanoscale cluster formation and percolative superconductivity in various cuprates<sup>29,30</sup>. Nanoscale spatial variations in the electronic characteristics have been observed in underdoped  $\text{Bi}_2\text{Sr}_2\text{CaCu}_2\text{O}_{8+\delta}$  with scanning tunneling microscopy<sup>31,32,33,34</sup>. They reveal a spatial segregation of the electronic structure into 3-nm-diameter superconducting domains in an electronically distinct background. Furthermore, the investigations of Gauzzi *et al.*<sup>35</sup> on  $\text{YBa}_2\text{Cu}_3\text{O}_{6.9}$  films with reduced long-range structural order clearly reveals that the size of the homogeneous domains strongly depends on the growth conditions. In any case we have shown that the analysis of reversible magnetization data taken near criticality does not uncover the critical properties of the associated fictitious homogeneous and infinite system only, but provides lower bounds for the extent of the homogeneous domains as well. Last but not least, having established the consistency with 3D-xy universality there are universal relations such as (4)-(6) and (10). They imply that the effect of pressure and isotope exchange on the respective properties are not independent.

The author is grateful to S. Salem-Sugui Jr. and J. R. Cooper for providing the magnetization data.

\* Electronic address: toni.schneider@physik.unizh.ch

<sup>1</sup> T. Schneider and J. M. Singer, *Phase Transition Approach To High Temperature Superconductivity*, (Imperial College Press, London, 2000).

<sup>2</sup> T. Schneider, in: *The Physics of Superconductors*, edited by K. Bennemann and J. B. Ketterson (Springer, Berlin, (2004), p. 111.

<sup>3</sup> T. Schneider, Phys. Rev. B **67**, 134514 (2003).

<sup>4</sup> M. A. Hubbard, M. B. Salamon, and B. W. Veal, Physica C **259**, 309 (1996).

<sup>5</sup> D. Babic, J. R. Cooper, J. W. Hodby, and Chen

Changkang, Phys. Rev. B **60**, 698 (1999).

<sup>6</sup> J. Hofer, T. Schneider, J. M. Singer, M. Willemin, H. Keller, T. Sasagawa, K. Kishio, K. Conder, and J. Karpinski, Rev. B **62**, 631 (2000).

<sup>7</sup> T. Schneider, Physica B **326**, 289 (2003).

<sup>8</sup> T. Schneider, R. Khasanov, K. Conder, E. Pomjakushina, R. Bruetsch, and H. Keller, J. Phys.: Condens. Matter **16**, L 437 (2004).

<sup>9</sup> Y. Ando and K. Segawa, Phys. Rev. Lett. **88**, 167005 (2002).

<sup>10</sup> S. Salem-Sugui Jr., A. D. Alvarenga, K. C. Goretta, V. N.

- Vieira, B. Veal, and A. P. Paulikas, Journ. Low Temp. Phys., **141**, 83 (2005).
- <sup>11</sup> S. Salem-Sugui Jr., A. D. Alvarenga, B. Veal, and A. P. Paulikas, J. Low. Temp. Phys. to be published.
  - <sup>12</sup> P. Zimmermann *et al.*, Phys. Rev. B **52**, 541 (1995).
  - <sup>13</sup> B. Janossy, D. Prost, S. Pekker, and L. Fruchter, Physica C **181**, 51 (1991).
  - <sup>14</sup> D. S. Fisher, M. P. A. Fisher and D. A. Huse, Phys. Rev. B **43**, 130 (1991).
  - <sup>15</sup> T. Schneider and D. Ariosi, Z. Phys. B **89**, 267 (1992).
  - <sup>16</sup> T. Schneider and H. Keller, Int. J. Mod. Phys. B **8**, 487 (1993).
  - <sup>17</sup> T. Schneider, J. Hofer, M. Willemin, J.M. Singer, and H. Keller, Eur. Phys. J. B **3**, 413 (1998).
  - <sup>18</sup> J. Hofer, T. Schneider, J. M. Singer, M. Willemin, H. Keller, C. Rossel, and J. Karpinski, Pys. Rev. B **60**, 1332 (1999).
  - <sup>19</sup> A. Peliasetto and E. Vicari, Physics Reports **368**, 549 (2002).
  - <sup>20</sup> R. E. Prange, Phys. Rev. B **1**, 2349 (1970).
  - <sup>21</sup> A. B. Harris, J. Phys. C **7**, 1671 (1974).
  - <sup>22</sup> J. L. Cardy ed., *Finite-Size Scaling*, North Holland, Amsterdam 1988.
  - <sup>23</sup> V. Privman, *Finite Size Scaling and Numerical Simulations of Statistical Systems*, World Scientific, NJ, 1990.
  - <sup>24</sup> A. Junod, J. Y. Genoud, G. Triscone, and T. Schneider, Physica C **294**, 115 (1998).
  - <sup>25</sup> V. Oganessian, D. A. Huse, and S. L. Sondhi, Phys. Rev. B **73**, 094503 (2006).
  - <sup>26</sup> D. R. Harshman and A. P. Millis, Phys. Rev. B **45**, 10684 (1992).
  - <sup>27</sup> T. Schneider and D. Di Castro, Phys. Rev. B **69**, 024502 (2004).
  - <sup>28</sup> G. Bednorz and K.A. Müller, Z. Phys. B: Condens. Matter **64**, 189 (1986).
  - <sup>29</sup> J. Mesot, P. Allensbach, U. Staub, and A. Furrer, Phys. Rev. Lett. **70**, 865 (1993).
  - <sup>30</sup> A. Furrer *et al.*, Physica C **235-240**, 261 (1994).
  - <sup>31</sup> J. Liu, J. Wan, A. Goldman, Y. Chang, and P. Jiang, Phys. Rev. Lett. **67**, 2195 (1991).
  - <sup>32</sup> A. Chang, Z. Rong, Y. Ivanchenko, F. Lu, and E. Wolf, Phys. Rev. B **46**, 5692 (1992).
  - <sup>33</sup> T. Cren, D. Roditchev, W. Sacks, J. Klein, J.-B. Moussy, C. Deville-Cavellin, and M. Laguës, Phys. Rev. Lett. **84**, 147 (2000).
  - <sup>34</sup> K.M. Lang, V. Madhavan, J.E. Hoffman, E.W. Hudson, H. Eisaki, S. Uchida, and J.C. Davis, Nature (London) **415**, 413 (2002).
  - <sup>35</sup> A. Gauzzi *et al.*, Europhys. Lett. **51**, 667, (2000).